A&A 590, A32 (2016)
DOI: 10.1051/0004-6361/201527848

Astronomy & Astrophysics

The Solar Twin Planet Search

III. The [Y/Mg] clock: estimating stellar ages of solar-type stars⋆

M. Tucci Maia[1], I. Ramírez[2], J. Meléndez[1], M. Bedell[3], J. L. Bean[3], and M. Asplund[4]

[1] Universidade de São Paulo, Departamento de Astronomia do IAG/USP, Rua do Matão 1226, Cidade Universitária, 05508-900 São Paulo, SP, Brazil
e-mail: marcelotuccimaia@usp.br
[2] University of Texas, McDonald Observatory and Department of Astronomy at Austin, Austin, TX 78712, USA
[3] University of Chicago, Department of Astronomy and Astrophysics, IL 60637,USA
[4] The Australian National University, Research School of Astronomy and Astrophysics, Cotter Road, Weston, ACT 2611, Australia

Received 26 November 2015 / Accepted 16 March 2016

ABSTRACT

Context. Solar twins are stars with similar stellar (surface) parameters to the Sun that can have a wide range of ages. This provides an opportunity to analyze the variation of their chemical abundances with age. Nissen (2015, A&A, 579, A52) recently suggested that the abundances of the s-process element Y and the α-element Mg could be used to estimate stellar ages.
Aims. This paper aims to determine with high precision the Y, Mg, and Fe abundances for a sample of 88 solar twins that span a broad age range (0.3–10.0 Gyr) and investigate their use for estimating ages.
Methods. We obtained high-quality *Magellan* Inamori Kyocera Echelle (MIKE) spectra and determined Y and Mg abundances using equivalent widths and a line-by-line differential method within a 1D LTE framework. Stellar parameters and iron abundances were measured in Paper I of this series for all stars, but a few (three) required a small revision.
Results. The [Y/Mg] ratio shows a strong correlation with age. It has a slope of -0.041 ± 0.001 dex/Gyr and a significance of 41σ. This is in excellent agreement with the relation first proposed by Nissen (2015). We found some outliers that turned out to be binaries where mass transfer may have enhanced the yttrium abundance. Given a precise measurement of [Y/Mg] with typical error of 0.02 dex in solar twins, our formula can be used to determine a stellar age with ~0.8 Gyr precision in the 0 to 10 Gyr range.

Key words. stars: abundances – stars: evolution – Galaxy: evolution

1. Introduction

Solar twins are stars that have spectra very similar to the Sun, with stellar (surface) parameters (temperature, surface gravity, and metallicity) around the solar values ($T_{\rm eff}$ within ±100 K, log g and [Fe/H] within ±0.1 dex, as arbitrarily defined in Ramírez et al. 2014)[1]. Since they have about 1 $M_{\odot}$ and roughly solar chemical composition, they follow a similar evolutionary path to the Sun, from the zero age main sequence to the end of their lives. The highly precise atmospheric parameters that one can derive for these objects allows a reliable determination of their ages using the traditional isochrone method (Ramírez et al. 2014; Nissen 2015). Thus, we can take advantage of this very special group of stars to better understand the nucleosynthesis of s- and r-elements throughout the Galaxy (e.g. Mashonkina & Gehren 2000; Battistini & Bensby 2016).

Another important potential application of the heavy elements is their use for age dating. By investigating the abundances of several elements using high precision differential abundances for a sample of 21 solar twins, Nissen (2015) finds a very tight correlation of [Y/Mg] as a function of stellar age. There have also been previous studies at standard precision that indicate a correlation between the s-process elements, like Ba and Y, with stellar age (Mashonkina & Gehren 2000; Bensby et al. 2005; D'Orazi et al. 2009). More recently, Maiorca et al. (2011) reinforced the above results using open clusters in a broad age range.

The aim of this work is to analyze the abundances of the heavy element yttrium and the α-element magnesium in a sample of 88 solar twins with ages covering 0.3 Gyr to 10.0 Gyr, which thus have important implications for astronomy, such as for dating exoplanet host stars, studying stellar evolution effects, Galactic chemical evolution, and different studies of stellar populations.

2. Data and analysis

2.1. Observations and data reduction

The observations for the 88 stars of our sample of solar twins were carried out with the *Magellan* Inamori Kyocera Echelle (MIKE) spectrograph (Bernstein et al. 2003) on the 6.5 m *Clay Magellan* Telescope at Las Campanas Observatory on five runs between January 2011 and May 2012. See Ramírez et al. (2014) for a more detailed description of our sample, the observations, and data reduction.

The same instrumental setup was employed for all stars, achieving a signal-to-noise ratio of at least 400 around 600 nm.

⋆ Based on observations obtained at the *Clay Magellan* Telescopes at Las Campanas Observatory, Chile and at the 3.6 m Telescope at the La Silla ESO Observatory, Chile (program ID 188.C-0265).
[1] We note that some stars in Ramírez et al. (2014) fall slightly outside the solar twin definition. They are also included in this work because they are close enough to the Sun for a high-precision abundance analysis.

The resolving power is $R = 83\,000$ in the blue, and $R = 65\,000$ in the red. The spectra of the Sun, which served as a reference for the differential analysis, were obtained through the observation of the asteroids Iris and Vesta using the same instrumentation setup[2]. The orders were extracted with the CarnegiePython MIKE pipeline[3], and Doppler correction and continuum normalization was performed with IRAF.

2.2. Stellar parameters

Stellar parameters were obtained by Ramírez et al. (2014) through differential excitation and ionization equilibrium using the abundances of FeI and FeII, with the Sun as reference. The abundances were determined using the line-by-line differential method, employing EW that were measured by hand with the task splot in IRAF. The Fe abundances and stellar parameters from Ramírez et al. (2014), were determined with the 2014 version of the LTE code MOOG (Sneden 1973), adopting the MARCS grid of 1D-LTE model atmospheres (Gustafsson et al. 2008). The Y and Mg abundances were determined with same grid, but we note that the exact grid of model atmospheres is irrelevant for differential abundances, since the mean abundance difference is lower than 0.001 dex (Meléndez et al. 2012). We have repeated our calculations using Kurucz ODFNEW model atmospheres (Castelli & Kurucz 2004) and found that the mean differential [Mg/H] and [Y/H] abundance change in only (Kurucz – MARCS) −0.0006 dex ($\sigma = 0.0031$) and –0.0003 dex ($\sigma = 0.0045$), respectively.

We also employed the recently introduced python q^2 code[4] (Ramírez et al. 2014), which makes the abundance determination and analysis considerably more efficient, by calling MOOG drivers and performing the line-by-line analysis, including corrections by hyperfine structure (HFS) and also computing the associated errors. Both observational and systematic uncertainties were considered. Observational errors are due to uncertainties in the measurements (standard error) while the systematic errors are uncertainties coming from the stellar parameters, as described in Ramírez et al. (2015). Observational and systematic errors were added in quadrature.

The age and mass for the sample were determined using Yonsei-Yale isochrones (Yi et al. 2001), as described in Ramírez et al. (2013, 2014). This method provides good relative ages, due to the high precision of the atmospheric parameters, by comparing the location of the star on the $T_{\rm eff}$, $\log g$, [Fe/H] parameter space, with the values predicted by the isochrones, computing mass, and age probability distribution functions. As shown below, these ages can also be made accurate (i.e. almost insensitive to the choice of models) by forcing different isochrone sets to reproduce the solar parameters exactly.

Figure 1 shows the location of the Sun in the $T_{\rm eff} - \log g$ plane along with 4.6 Gyr Yonsei-Yale (YY) and 4.5 Gyr Darmouth (DM) isochrones (Dotter et al. 2008). These ages are the closest to solar age found in each grid. Solid lines represent the isochrones of solar composition in each case. Clearly, they do not exactly pass through the solar location, but a minor shift of the [Fe/H] of the isochrone sets by –0.04 in the case of YY (dashed line) and +0.08 for DM (dot-dashed line) brings these isochrones to excellent agreement with the solar

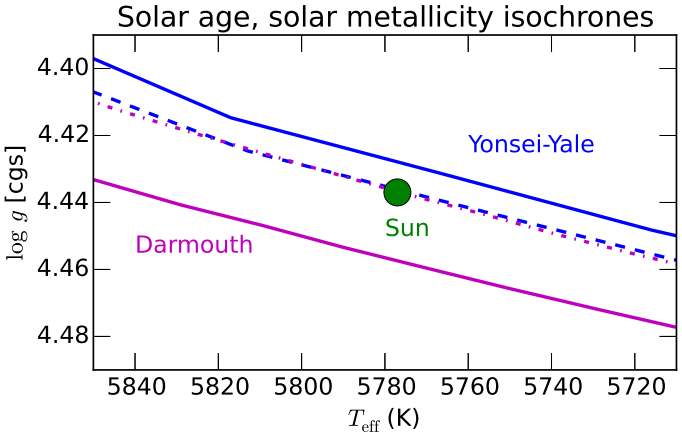

Fig. 1. The 4.6 Gyr Yonsei-Yale (dashed line) and 4.5 Gyr Darmouth (dot-dashed line) isochrones shifted in [Fe/H] by –0.04 dex and +0.08 dex, respectively. We note the agreement after the change.

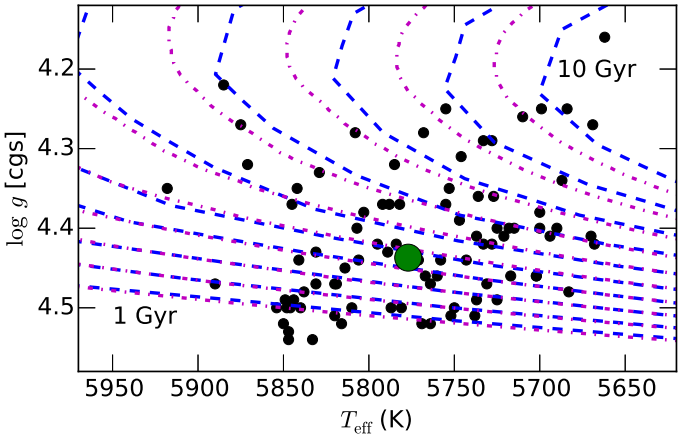

Fig. 2. Distribution of our sample with the 1 to 10 Gyr Yonsei-Yale (dashed lines) and Darmouth (dot-dashed lines) isochrones.

parameters at the well-known solar age (e.g. Sackmann et al. 1993). We applied these offsets to both isochrone grids before using them to determine stellar parameters[5].

As shown in Fig. 2, our solar twin data set spans a narrow range of $T_{\rm eff}$ and $\log g$, but it is enough to cover the very wide range of ages from 0 to 10 Gyr. YY (dashed lines) and DM (dot-dashed lines) isochrones are also shown in this plot. These isochrones have [Fe/H] = −0.04 for Yonsei-Yale and [Fe/H] = +0.08 for DM, which, as explained above, pass through the solar location at solar age. We note the excellent agreement between these two sets of isochrones for ages younger than 6 Gyr. For older stars, the DM isochrones are shifted to somewhat higher effective temperatures, which implies that the ages inferred from them will be somewhat older, compared to those obtained from the Yonsei-Yale set.

[2] In this work we only use the light reflected on Iris as our reference spectrum for the differential analysis.
[3] http://code.obs.carnegiescience.edu/mike
[4] https://github.com/astroChasqui/q2; a tutorial is available on this site with detailed information on the capabilities of this code.

[5] In R14, the –0.04 dex offset in the YY isochrone [Fe/H] values was applied after selecting the isochrone points to use in the probability density (PD) calculations. This led to a very minor offset (−0.1 ± 0.2 Gyr) in the ages derived with respect to the more precise case where the isochrone [Fe/H] values are all shifted before selecting the points to use in the PD computation. This minor change makes the ages reported in R14 slightly different from those employed in this work, but these small differences do not affect the results presented in this paper in any significant way.

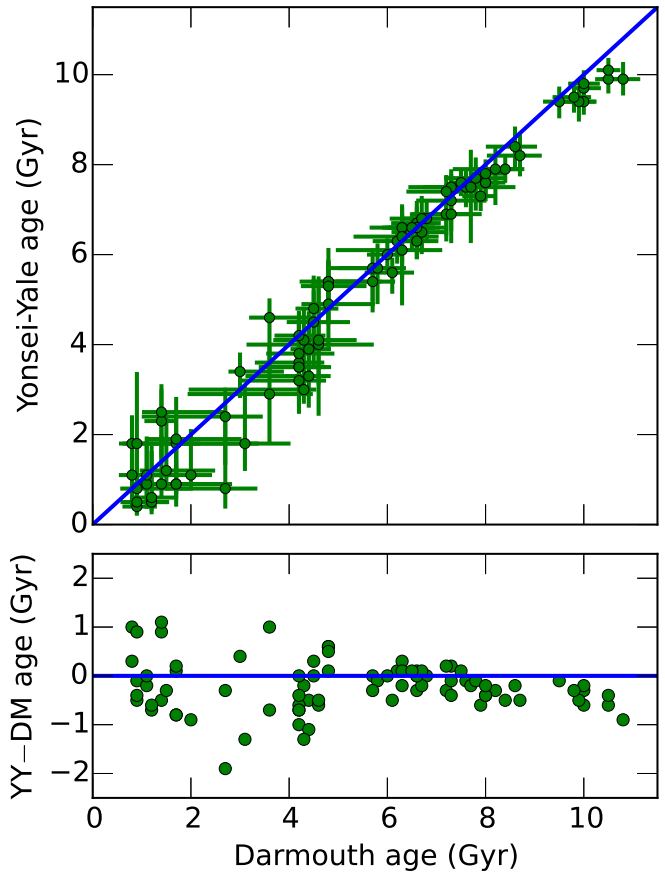

Fig. 3. *Upper panel*: comparison of ages estimated by Yonsei-Yale and Darmouth isochrones for our solar twin sample. *Lower panel*: differences between the YY and DM isochronal ages.

Figure 3 compares the YY and DM isochrone ages derived for our solar twin stars. On average, the mean difference of the most probable ages (DM–YY) is +0.2 ± 0.5 Gyr, which would suggest good agreement within the errors. However, there is a clear systematic offset at older ages, albeit small, of +0.4 ± 0.2 Gyr.

If the [Fe/H] offsets to the isochrones are not applied, the YY and DM isochrones are systematically off by 1 Gyr at solar age, and up to 2 Gyr for the oldest stars. On the other hand, when these corrections are applied to the isochrones, the anchor points are the solar parameters, which give us relative accurate ages. We note that, for the pair of old solar twins 16 Cyg, our method gives an age of $7.1^{+0.2}_{-0.4}$ Gyr (from the combined age-probability distributions; Ramírez et al. 2011), which is in excellent agreement with the seismic ages recently determined for this pair (average of 7.0 ± 0.1 Gyr; van Saders et al. 2016). Even though the typical error for both isochronal ages set is ∼0.6 Gyr, we decided to use the YY grid instead of DM because the former has a more consistent sampling of the isochrones, which makes the age determination less likely to suffer from statistical biases.

The stellar parameters and [Fe/H] abundances for most of our sample stars were determined in our previous work (Ramírez et al. 2014), except for HIP 108158, HIP 55409, HIP 72043, and HIP 68468. As these stars were outliers in the [Y/Mg] versus age plot (there are other outliers, but they can be explained owing to to binarity), we decided to verify their parameters by remeasuring the EW of FeI and FeII lines for those stars (the reanalysis of HIP 68468 is presented in Meléndez et al. 2016). For HIP 72043, we didn't find any difference, meaning that it is a true outlier in the [Y/Mg]-age plane; for the other three stars, their parameters were revised (Table 1).

Table 1. Revised parameters for HIP 108158, HIP 55409, and HIP 68468.

Star HIP	$T_{\rm eff}$ (K)	$\log g$ (dex)	[Fe/H] (dex)	Mass ($M_\odot$)	Age (Gyr)
108158	5688 ± 6	4.29 ± 0.02	0.067 ± 0.008	$0.99^{1.01}_{0.98}$	$9.0^{+0.4}_{-.4}$
55409	5712 ± 6	4.41 ± 0.02	–0.060 ± 0.006	$0.96^{0.97}_{0.95}$	$6.9^{+0.7}_{-0.7}$
68468	5857 ± 8	4.32 ± 0.02	0.065 ± 0.007	$1.05^{1.06}_{1.04}$	$5.9^{+0.4}_{-0.4}$

We also updated the ages for HIP 109110 and HIP 29525, two young solar twins, for which more precise ages, which were determined through rotational periods, are available in Baumann et al. (2010)[6]. According to Barnes (2007), the errors from gyrochronology is 15% in the age of solar analogs, which is significantly better than those found in Ramírez et al. (2014), which are about 40–70% for these two young stars (isochrone ages have larger error bars at a younger age, as seen in Fig. 3). We note also that, for those two stars, the rotational ages agree better with the [Y/Mg] ages.

2.3. Abundance analysis

Yttrium abundances were obtained using the 485.48 nm, 520.04 nm, and 540.27 nm YII lines and corrected for HFS adopting the HFS data from Meléndez et al. (2012).

For magnesium we used the 454.11 nm, 473.00 nm, 571.11 nm, 631.87 nm, and 631.92 nm lines, paying extra attention to the latter two lines owing to the influence of telluric features in this region, as shown in Fig. 4. We note that the separation between theses telluric lines is 0.74 Å and their line ratio is 1.05.

Once the initial set of differential abundances was obtained, we verified the presence of outliers and, when present, the EW of those lines were verified and q^2 was executed again.

3. Results and discussions

As shown in Fig. 5, there is a clear correlation between both [Y/Fe] and [Mg/Fe], and stellar age, for the sample of 88 stars, confirming the result found by Nissen (2015), which is based on a smaller sample. The behaviour of yttrium is due to the increasing contribution of s-process elements from low and intermediate mass AGB stars, which most efficiently produce Y (Fishlock et al. 2014; Karakas & Lattanzio 2014) and which slowly became more important with time (Travaglio et al. 2004; Nissen 2015).

On the other hand, the correlation of [Mg/Fe] with age is an effect of the increasing number of Type Ia SNe in comparison to the number of Type II SNe, as discussed by Kobayashi et al. (2006). This is because Type II SNe produces mainly α-elements (O, Mg, Si, S, Ca, and Ti), enhancing the interstellar medium with these species in the early Galaxy, while Type Ia SNe produce yields with high Fe/α ratio. Complementary to this, we show with the [Fe/H] vs. age plot that there is no age-metallicity correlation for the stars in our data, independently of its population (Fig. 5).

[6] We note that HIP 109110 is not used in the linear fit because it was identified as a spectroscopic binary. For HIP 29525, even if we adopt the more uncertain isochronal age, the linear fit is not changed because of the large error bar in age for this star.

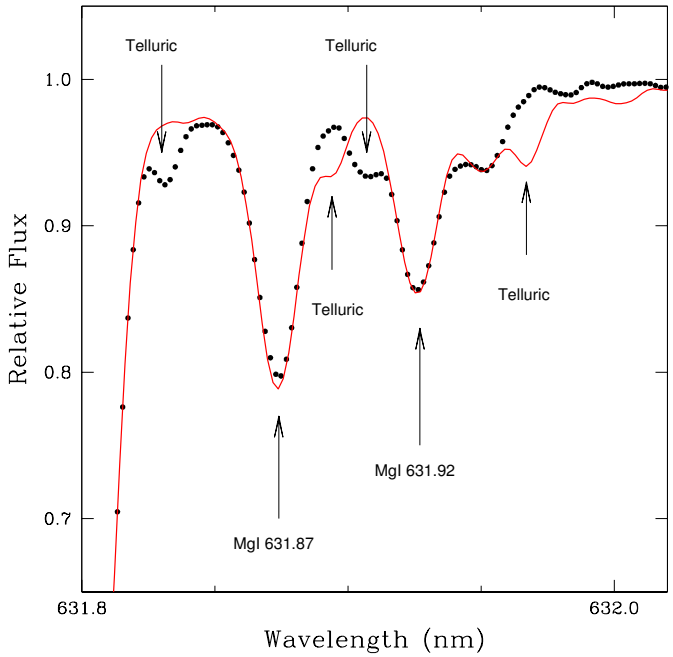

Fig. 4. Mg I lines around 631.9 nm and telluric lines in this region for HIP 64713 (black dots) and HIP 89650 (red line). We advise caution swhen measuring these Mg I lines.

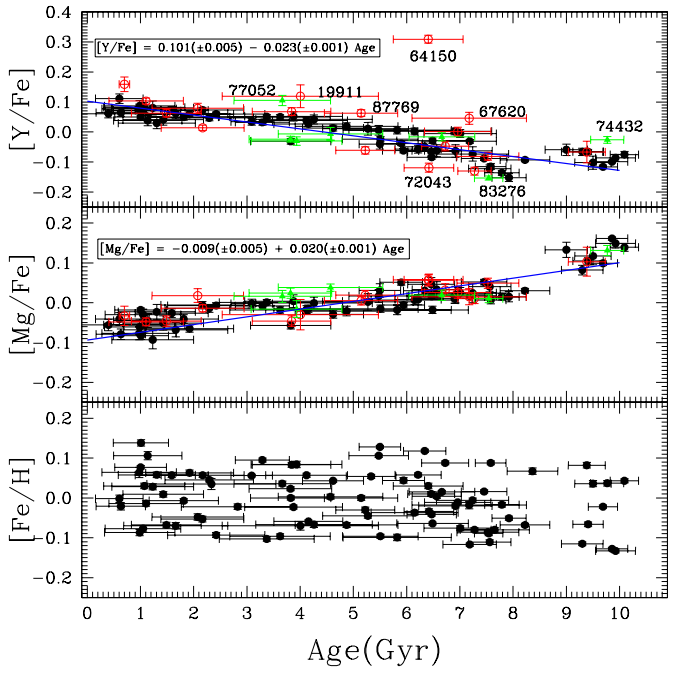

Fig. 5. [Y/Fe] (*upper panel*), [Mg/Fe] (*middle panel*), and [Fe/H] (*lower panel*) as function of age. The red open circles are spectroscopic binary stars and the green triangles are visual binaries. [Fe/H] vs. age do not show any correlation with age. We also present the linear fit for [Y/Fe] and [Mg/Fe] versus age on their respective panels.

In Fig. 5, there is a gap around 8.5 Gyr that could be important when distinguishing different populations. This gap in the [Mg/Fe] vs. age plot was used to identify 10 stars that display a high-α abundance that, according to Haywood et al. (2013), may belong to the thick disk population. On the other hand, Adibekyan et al. (2011) classify these high-α metal-rich stars (hαmr) as being a different population of stars, that do not belong

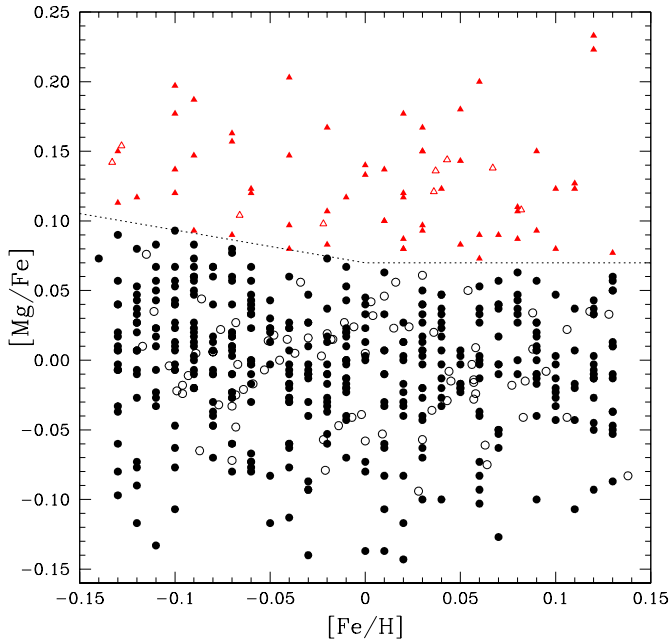

Fig. 6. [Mg/Fe] vs. [Fe/H] plot of the data from Adibekyan et al. (2012; filled symbols) matching the [Fe/H] range from our work (empty points). The circles represents the thin disk stars and the triangles the hαmr stars.

to either the thin or the thick disk. These stars share some properties with both thin and thick disks stars and might have migrated from the inner parts of the Galaxy (Adibekyan et al. 2013). However the detailed study of these stars by Haywood et al. (2013) indicates that they may have formed at the end of the thick disk.

Using the Adibekyan et al. (2013) criteria, nine stars from our sample are hαmr (Fig. 6)[7]. With this method, we identify the same hαmr stars as we did using the [Mg/Fe] vs. age plot (Fig. 5), with the exception of HIP 109821. Adopting a binomial distribution (e.g. Bevington 1969, Chap. 3). the occurrence of hαmr in our sample is 10/88 (11.4 ± 3.4%) which is consistent with the 3/21 (14.3 ± 7.6%) from Nissen (2015) and 60/413 (14.5 ± 1.7%) from Adibekyan et al. (2012), using the same metallicity range of our sample.

We also show the Toomre diagram for the sample (Fig. 7) highlighting the hαmr stars (open circles). The hαmr group does not seem to be particularly separated from the rest of the group and its kinematic properties are in agreement with the findings by Adibekyan et al. (2011, 2013), as well as Bensby et al. (2014).

The red open circles on the [Y/Fe] and [Mg/Fe] plots (and in Fig. 9) are binaries, pinpointed through radial velocity changes. The majority of the stars from our MIKE sample overlap with our HARPS Large Program (Ramírez et al. 2014), in which we search for exoplanets in a sample of about 60 solar twins using the HARPS spectrograph (Mayor et al. 2003). Thanks to the radial velocity data of our sample (and previous works), we identified some binary or multiple system stars (red open circles), indicated in Table A.1. From our visual inspection, all spectroscopic binaries seem single-lined. Also, the single-lined nature of the spectra is apparent in the iron abundance analysis; the EWs do not appear to be contaminated in any significant manner.

[7] Using data from Adibekyan et al. (2012), that matches the range of metallicities of our sample (–0.140 to 0.140 dex). Notice that we use [Mg/Fe] rather than [α/Fe] (which is the average of Mg, Si and Ti).

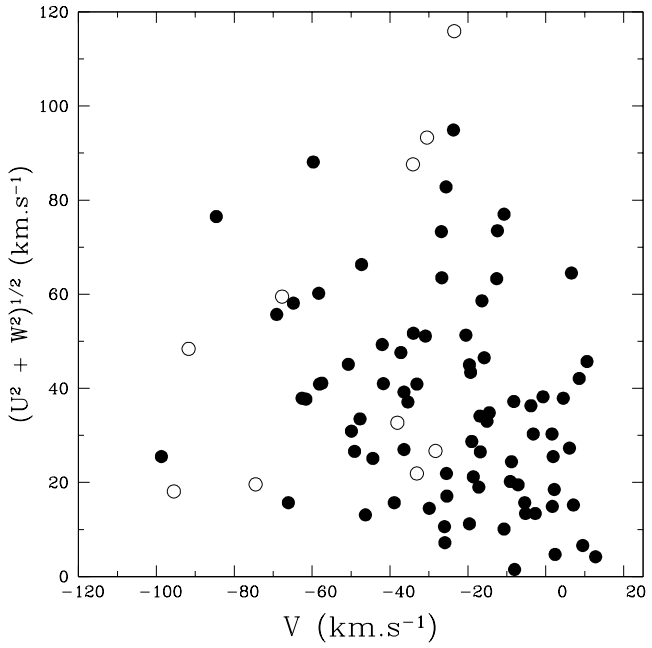

Fig. 7. Toomre diagram for our sample. The open circles are the high-α metal rich star stars.

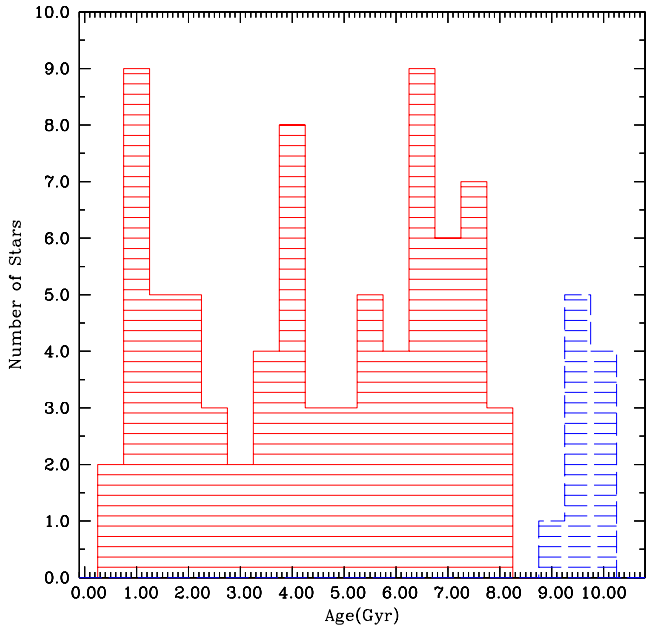

Fig. 8. Age histogram for the thin disk (red solid line) and hαmr stars (blue dashed line).

We also note that in the [Y/Fe] plot, all outliers are spectroscopic binaries (red open dots). This is probably because their companion transfered Y material to what is now the primary star. Thus, [Y/Fe] seems to be a good method to identify potential multiple star systems where mass transfer has taken place, but this is possible only when precise ages are available. We note that the stars HIP 77052, HIP 74432, and HIP 83276, which seem to be outliers in the [Y/Fe] plot, are identified as visual binaries (Tokovinin 2014).

Figure 8 shows an age histogram of the whole sample. The red solid curve shows the thin disk, while the blue dashed line represents the stars assigned to the hαmr population. It is possible to distinguish a clear age gap at 8.0 Gyr, separating the thin disk and the hαmr stars. The hαmr population show a star-to-star scatter in age of only 0.3 Gyr, showing that this population formed quickly. Nevertheless, the hαmr stars cover an [Fe/H] range similar to that of the younger thin disk stars that formed during the last 8 Gyr.

In Fig. 9 we present the [Y/Mg] vs. stellar age plot. A linear fit to our data, excluding the spectroscopic and visual binary stars, gives the following relation using the YY ages[8]:

$$[Y/Mg] = 0.186(\pm0.008) - 0.041(\pm0.001).Age. \quad (1)$$

This is practically the same fit found by Nissen (2015), within 1σ, but with better precision and a scatter of 0.037 dex. A remarkable significance level of about 41σ is found for the slope and a Spearman coefficient of $r_S = -0.96$, with a probability of 10^{-35} of our results arising by pure chance, showing that this behaviour cannot occur randomly. We note that the hαmr stars were not excluded from the fit, meaning hat the [Y/Mg] relation seems to also be valid for this population. The relation of age (in Gyr) as function of [Y/Mg] is

$$Age = 4.50(\pm0.09) - 24.18(\pm0.66).[Y/Mg]. \quad (2)$$

[8] We have made tests using DM and YY ages with [Y/Mg] abundances to identify which would have the better fit with age, but we found the same scatter (0.038 dex in [Y/Mg]) and the same slope within 1σ. Since the differences in the age determination are small, they do not affect the final result.

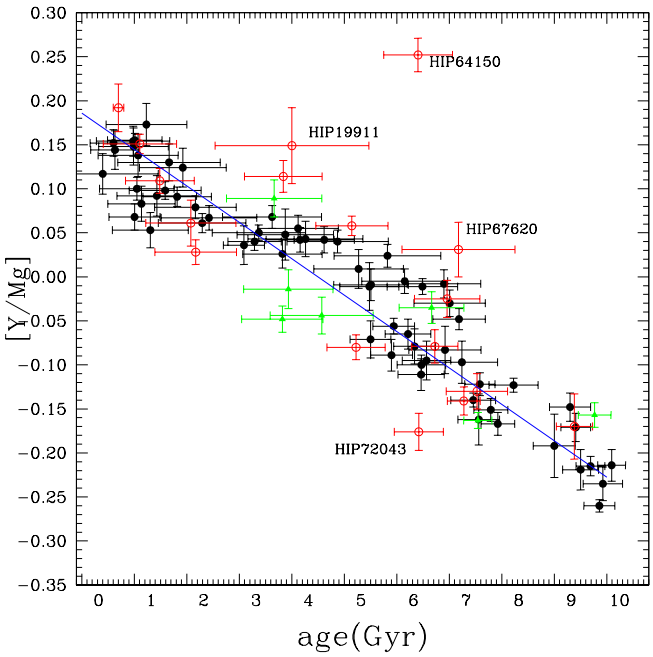

Fig. 9. [Y/Mg] versus age for the sample for 88 solar twins. The slope is $-4.13 \times 10^{-2} \pm 1.12 \times 10^{-3}$ with a scatter in age of 0.9 Gyr. The red open circles are spectroscopic binary stars and the green triangles are visual binaries.

The scatter of this relation is 0.9 Gyr, which is larger then the average error of the isochronal ages (0.6 Gyr). Subtracting these errors, we find an intrinsic uncertainty of 0.7 Gyr for the age determination (this value should be added to the error in the age determination from Eq. (1). For [Y/Mg], we have a mean error of 0.017 dex, which translates to a typical error in age of 0.4 Gyr. Thus, the total error expected is ~0.8 Gyr for data with quality similar to the those employed in this work.

The age – [Y/Mg] relation shown in Fig. 9 and described by Eqs. (1) and (2) was determined using a sample of solar twins for which highly precise Y and Mg abundances, as well as ages,

could be derived. Its origin is explained by nucleosynthesis and the chemical evolution of the solar neighbourhood. Thus, we do not expect this relation to be restricted to solar twins. Since nucleosynthetic yields can be metallicity-dependent, it is possible that this relation could be different for samples with non-solar [Fe/H]. We tested this possibility by dividing our sample into metal-rich and metal-poor groups, finding no significant differences. Thus, it is possible that the metallicity dependency is mild, if it is present at all. This means that, at least for the metallicity interval of our sample, the [Fe/H] does not have an impact on the age determination using Eq. (2). However, more studies are needed to determine if this remains true to metallicities other than solar. The [Y/Mg] abundance ratio can be measured with a precision of about 0.05 dex in non-solar twins. Our Eq. (2) can be used on those stars to determine their ages with a precision of 1.4 Gyr. With less precise [Y/Mg] measurements, for example assuming errors of 0.1 dex, we can still constrain the stellar age to 2.5 Gyr.

4. Conclusions

We confirm the tight relation of [Y/Mg] vs. age, first found by Nissen (2015). This relation seems to apply even for the thick disk population. Although we used a bigger sample of solar twins, the relation found is practically the same as Nissen's, with a slope of -0.041 ± 0.001 dex/Gyr and a scatter in ages of $\sigma = 0.9$ Gyr.

The mean uncertainty expected for data with precision similar to ours is ~0.8 Gyr. This level of precision for the abundances, stellar parameters, and age determination as well, could only be achieved through a strict differential analysis of solar twin stars. We note that our careful work allowed us to find a good correlation of [Y/Mg] abundances with stellar age. However, extremely high-precision abundances are not necessary to have a satisfactory age determination. Even with a [Y/Mg] ratio with error of 0.05 dex, it is possible to obtain an age with a uncertainty of 1.4 Gyr.

Tests were made to verify if this relation has some dependence with metallicity. For this we divided the group into metal-poor and metal-rich stars, but no significant trend with [Fe/H] was detected, meaning that the age determination, at least in the $-0.14 \leq$ [Fe/H] ≤ 0.14 dex interval, should not be metallicity-correlated.

More investigation is needed to verify the applicability of the [Y/Mg] clock relation to stars with metallicities that are different from solar. Also, this correlation may be more complex than just a simple linear fit. Nevertheless, with regard to solar twins and solar analogs, the [Y/Mg] ratio is a promising new metric to reliably estimate relative ages independent of isochrones, and could be used alongside other age determination methods.

Our work provides important observational constraints to the yields of s-process elements in models of low- and intermediate-mass AGB stars (e.g. Maiorca et al. 2012).

Acknowledgements. M.T.M. thanks support by CNPq (142437/2014-0). J.M. thanks for support by FAPESP (2012/24392-2). M.A. has been supported by the Australian Research Council (grants FL110100012 and DP120100991). M.B. is supported by the National Science Foundation (NSF) Graduate Research Fellowships Program (grant No. DGE-1144082). J.B. and M.B. acknowledge support for this work from the NSF (grant No. AST-1313119). J.B. is also supported by the Alfred P. Sloan Foundation and the David and Lucile Packard Foundation.

References

Adibekyan, V. Z., Santos, N. C., Sousa, S. G., & Israelian, G. 2011, A&A, 535, L11
Adibekyan, V. Z., Sousa, S. G., Santos, N. C., et al. 2012, A&A, 545, A32
Adibekyan, V. Z., Figueira, P., Santos, N. C., et al. 2013, A&A, 554, A44
Barnes, S. A. 2007, ApJ, 669, 1167
Battistini, C., & Bensby, T. 2016, A&A, 586, A49
Baumann, P., Ramírez, I., Meléndez, J., Asplund, M., & Lind, K. 2010, A&A, 519, A87
Bensby, T., Feltzing, S., Lundström, I., & Ilyin, I. 2005, A&A, 433, 185
Bensby, T., Feltzing, S., & Oey, M. S. 2014, A&A, 562, A71
Bevington, P. R. 1969, Data reduction and error analysis for the physical sciences (New York: McGraw-Hill)
Bernstein, R., Shectman, S. A., Gunnels, S. M., Mochnacki, S., & Athey, A. E. 2003, Proc. SPIE, 4841, 1694
Castelli, F., & Kurucz, R. L. 2004, ArXiv e-prints [arXiv:astro-ph/0405087]
D'Orazi, V., Randich, S., Flaccomio, E., et al. 2009, A&A, 501, 973
Dotter, A., Chaboyer, B., Jevremović, D., et al. 2008, ApJS, 178, 8
Fishlock, C. K., Karakas, A. I., Lugaro, M., & Yong, D. 2014, ApJ, 797, 44
Gustafsson, B., Edvardsson, B., Eriksson, K., et al. 2008, A&A, 486, 951
Haywood, M., Di Matteo, P., Lehnert, M. D., Katz, D., & Gómez, A. 2013, A&A, 560, A109
Karakas, A. I., & Lattanzio, J. C. 2014, PASA, 31, e030
Kobayashi, C., Umeda, H., Nomoto, K., Tominaga, N., & Ohkubo, T. 2006, ApJ, 653, 1145
Maiorca, E., Randich, S., Busso, M., Magrini, L., & Palmerini, S. 2011, ApJ, 736, 120
Maiorca, E., Magrini, L., Busso, M., et al. 2012, ApJ, 747, 53
Mashonkina, L., & Gehren, T. 2000, A&A, 364, 249
Gail, H.-P. 2009, Landolt Börnstein, 44
Mayor, M., Pepe, F., Queloz, D., et al. 2003, The Messenger, 114, 20
Meléndez, J., Bergemann, M., Cohen, J. G., et al. 2012, A&A, 543, A29
Meléndez, J., Bedell, M., Bean, L. J., et al. 2016, A&A, submitted
Nissen, P. E. 2015, A&A, 579, A52
Ramírez, I., Meléndez, J., Cornejo, D., Roederer, I. U., & Fish, J. R. 2011, ApJ, 740, 76
Ramírez, I., Allende Prieto, C., & Lambert, D. L. 2013, ApJ, 764, 78
Ramírez, I., Meléndez, J., Bean, J., et al. 2014, A&A, 572, A48
Ramírez, I., Khanal, S., Aleo, P., et al. 2015, ApJ, 808, 13
Sackmann, I.-J., Boothroyd, A. I., & Kraemer, K. E. 1993, ApJ, 418, 457
van Saders, J. L., Ceillier, T., Metcalfe, T. S., et al. 2016, Nature, 529, 181
Sneden, C. A. 1973, Ph.D. Thesis
Tokovinin, A. 2014, AJ, 147, 86
Travaglio, C., Gallino, R., Arnone, E., et al. 2004, ApJ, 601, 864
Yi, S., Demarque, P., Kim, Y.-C., et al. 2001, ApJS, 136, 417

Appendix A

Table A.1. [Y/H], [Mg/H], stellar parameters, and age for the 88 solar twins sample.

Star	[Y/H]	Error	[Mg/H]	Error	[Fe/H]	Error	$T_{\rm eff}$	Error	$\log g$	Error	Age	Error
HIP 10175	0.043	0.010	–0.048	0.005	–0.007	0.005	5738	7	4.51	0.01	1.815	0.652
HIP 101905	0.129	0.009	0.031	0.005	0.057	0.006	5890	6	4.47	0.02	1.589	0.685
HIP 102040	–0.033	0.006	–0.100	0.013	–0.093	0.006	5838	6	4.48	0.02	2.423	0.912
HIP 102152	–0.083	0.020	0.000	0.018	–0.020	0.005	5718	5	4.40	0.02	6.918	0.689
HIP 10303	0.112	0.016	0.123	0.022	0.106	0.004	5725	4	4.40	0.01	5.477	0.561
HIP 103983*	0.031	0.014	–0.030	0.020	–0.048	0.008	5752	10	4.51	0.02	2.077	0.859
HIP 104045	0.092	0.010	0.031	0.006	0.045	0.005	5831	6	4.47	0.02	2.293	0.833
HIP 105184	0.109	0.013	–0.043	0.008	–0.002	0.009	5833	11	4.504	0.02	0.604	0.445
HIP 108158	0.008	0.017	0.200	0.031	0.067	0.008	5687	7	4.34	0.02	8.364	0.477
HIP 108468	–0.233	0.011	–0.071	0.026	–0.111	0.006	5829	7	4.33	0.02	7.562	0.397
HIP 108996	0.141	0.009	–0.013	0.014	0.064	0.013	5847	17	4.503	0.03	0.978	0.700
HIP 109110*	0.194	0.018	0.002	0.019	0.035	0.014	5787	17	4.50	0.04	2.335	1.212
HIP 109821	–0.181	0.010	–0.033	0.011	–0.115	0.005	5746	7	4.31	0.02	9.301	0.390
HIP 114615	–0.007	0.011	–0.107	0.007	–0.077	0.008	5816	9	4.52	0.02	1.050	0.710
HIP 115577	–0.066	0.020	0.153	0.012	0.036	0.008	5699	9	4.25	0.03	9.501	0.342
HIP 116906	–0.055	0.017	0.056	0.009	0.010	0.005	5792	6	4.37	0.02	6.463	0.441
HIP 117367	–0.018	0.003	0.038	0.009	0.044	0.007	5871	8	4.32	0.02	5.942	0.395
HIP 118115	–0.153	0.007	–0.002	0.011	–0.017	0.006	5808	7	4.28	0.02	7.791	0.324
HIP 11915	–0.032	0.006	–0.074	0.011	–0.059	0.004	5760	4	4.46	0.01	4.157	0.647
HIP 14501	–0.219	0.010	0.016	0.015	–0.133	0.005	5728	7	4.29	0.02	9.926	0.374
HIP 14614	–0.093	0.009	–0.117	0.010	–0.099	0.008	5784	9	4.42	0.03	5.823	1.016
HIP 14623	0.144	0.013	0.061	0.013	0.106	0.01	5769	13	4.52	0.02	1.137	0.642
HIP 15527	–0.203	0.010	–0.036	0.005	–0.051	0.005	5785	5	4.32	0.01	7.924	0.320
HIP 18844	–0.072	0.007	0.068	0.005	0.016	0.004	5736	5	4.36	0.02	7.456	0.427
HIP 1954	–0.049	0.010	–0.089	0.009	–0.068	0.006	5717	5	4.46	0.02	4.872	0.965
HIP 19911*	0.049	0.035	–0.100	0.023	–0.070	0.011	5764	12	4.47	0.04	4.004	1.466
HIP 21079	–0.008	0.016	–0.138	0.014	–0.070	0.008	5846	11	4.50	0.03	1.663	0.977
HIP 22263	0.112	0.014	–0.026	0.019	0.030	0.007	5840	8	4.50	0.02	1.074	0.762
HIP 22395**	0.054	0.012	0.068	0.020	0.084	0.008	5789	8	4.43	0.02	3.934	0.853
HIP 25670	0.095	0.010	0.040	0.012	0.057	0.005	5771	5	4.44	0.02	4.120	0.768
HIP 28066	–0.227	0.001	0.033	0.006	–0.128	0.004	5733	5	4.29	0.01	9.859	0.295
HIP 29432	–0.120	0.007	–0.111	0.017	–0.096	0.005	5758	5	4.44	0.01	5.508	0.710
HIP 29525	0.039	0.012	–0.078	0.019	–0.022	0.007	5737	7	4.49	0.02	2.827	1.056
HIP 30037*	–0.010	0.015	0.015	0.015	–0.011	0.004	5668	5	4.42	0.01	6.960	0.624
HIP 30158	–0.003	0.021	0.041	0.007	0.003	0.006	5702	5	4.46	0.02	4.570	0.981
HIP 30344	0.122	0.006	–0.002	0.021	0.063	0.007	5750	9	4.50	0.02	1.924	0.826
HIP 30476	–0.138	0.005	0.077	0.010	–0.022	0.004	5710	5	4.26	0.01	9.689	0.273
HIP 30502	–0.081	0.014	–0.051	0.009	–0.076	0.006	5721	6	4.41	0.02	7.007	0.679
HIP 3203	0.000	0.015	–0.148	0.014	–0.087	0.008	5850	10	4.52	0.02	0.987	0.662
HIP 33094	–0.032	0.010	0.182	0.016	0.043	0.005	5662	7	4.16	0.02	10.092	0.265
HIP 34511	–0.052	0.003	–0.102	0.008	–0.103	0.006	5819	6	4.47	0.02	3.373	0.889
HIP 36512	–0.148	0.005	–0.100	0.010	–0.117	0.004	5737	4	4.41	0.01	7.185	0.500
HIP 36515	0.044	0.009	–0.100	0.019	–0.021	0.009	5847	12	4.54	0.02	0.633	0.464
HIP 38072	0.088	0.018	0.035	0.009	0.058	0.007	5849	8	4.49	0.02	1.306	0.724
HIP 40133	0.088	0.018	0.159	0.012	0.128	0.004	5755	4	4.37	0.01	5.500	0.389
HIP 41317	–0.161	0.004	–0.038	0.005	–0.068	0.004	5700	5	4.38	0.01	8.224	0.468
HIP 42333	0.210	0.006	0.055	0.007	0.138	0.008	5848	8	4.50	0.02	1.011	0.518
HIP 43297*	0.151	0.011	0.037	0.014	0.083	0.006	5702	5	4.46	0.01	3.840	0.738
HIP 44713	–0.027	0.010	0.095	0.009	0.088	0.005	5768	6	4.28	0.01	7.581	0.288
HIP 44935	0.001	0.013	0.066	0.012	0.058	0.005	5782	5	4.37	0.01	6.215	0.434
HIP 44997	0.029	0.016	–0.019	0.025	–0.023	0.005	5731	5	4.47	0.02	3.876	0.919
HIP 4909	0.108	0.021	–0.065	0.011	0.028	0.008	5854	10	4.50	0.02	1.232	0.770
HIP 49756	0.056	0.008	0.014	0.012	0.043	0.004	5795	4	4.42	0.01	4.618	0.573
HIP 5301	–0.093	0.009	–0.082	0.003	–0.064	0.004	5728	5	4.42	0.02	6.488	0.670
HIP 54102*	0.089	0.007	–0.062	0.008	–0.014	0.007	5820	9	4.51	0.02	1.107	0.698
HIP 54287	0.069	0.015	0.148	0.013	0.118	0.004	5727	4	4.36	0.01	6.340	0.398

Notes. The binary stars are identified by *. (*) Spectroscopic binary star. (**) Visual binary star.

Table A.1. continued.

Star	[Y/H]	Error	[Mg/H]	Error	[Fe/H]	Error	T_{eff}	Error	log g	Error	Age	Error
HIP 54582*	–0.210	0.011	–0.069	0.011	–0.080	0.005	5875	7	4.27	0.02	7.276	0.312
HIP 55409	–0.078	0.009	–0.070	0.014	–0.080	0.006	5700	6	4.40	0.02	7.655	0.650
HIP 62039*	0.041	0.016	0.120	0.010	0.088	0.005	5753	6	4.35	0.02	6.725	0.441
HIP 6407*	–0.005	0.011	–0.114	0.009	–0.068	0.007	5764	8	4.52	0.01	1.488	0.656
HIP 64150*	0.339	0.011	0.087	0.015	0.030	0.007	5747	6	4.39	0.02	6.406	0.656
HIP 64673*	–0.091	0.009	–0.011	0.010	–0.030	0.007	5918	8	4.35	0.02	5.224	0.554
HIP 64713	–0.025	0.014	–0.068	0.015	–0.067	0.007	5767	8	4.46	0.02	4.261	1.096
HIP 65708	–0.132	0.005	0.039	0.016	–0.066	0.006	5755	6	4.25	0.02	9.410	0.284
HIP 67620*	0.028	0.017	–0.003	0.016	–0.018	0.009	5670	9	4.41	0.03	7.176	1.077
HIP 68468	0.016	0.005	0.105	0.016	0.054	0.005	5845	6	4.37	0.02	5.334	0.467
HIP 69645	–0.034	0.020	–0.043	0.010	–0.045	0.006	5743	6	4.44	0.02	5.273	0.852
HIP 72043*	–0.153	0.014	0.023	0.015	–0.034	0.007	5842	8	4.35	0.02	6.419	0.468
HIP 73241*	0.015	0.036	0.185	0.011	0.082	0.007	5669	8	4.27	0.02	9.384	0.346
HIP 73815	–0.058	0.018	0.037	0.011	0.004	0.005	5788	6	4.37	0.02	6.566	0.462
HIP 74389	0.127	0.003	0.059	0.015	0.077	0.004	5844	5	4.49	0.01	1.005	0.484
HIP 74432**	0.011	0.009	0.168	0.011	0.037	0.007	5684	8	4.25	0.02	9.768	0.312
HIP 7585	0.127	0.009	0.087	0.005	0.095	0.005	5831	5	4.43	0.01	3.291	0.508
HIP 76114	–0.035	0.010	–0.030	0.011	–0.037	0.006	5733	6	4.42	0.02	6.151	0.816
HIP 77052**	0.141	0.016	0.052	0.013	0.036	0.006	5683	5	4.48	0.02	3.665	0.906
HIP 77883	–0.079	0.024	0.018	0.008	–0.006	0.006	5690	6	4.4	0.02	7.240	0.678
HIP 79578*	0.071	0.008	0.043	0.012	0.057	0.005	5820	5	4.47	0.01	2.170	0.778
HIP 79672	0.090	0.010	0.054	0.019	0.056	0.003	5814	3	4.45	0.01	3.090	0.391
HIP 79715	–0.125	0.004	–0.025	0.010	–0.041	0.005	5803	6	4.38	0.02	6.471	0.462
HIP 81746*	–0.167	0.012	–0.037	0.016	–0.086	0.004	5715	5	4.40	0.02	7.526	0.582
HIP 83276**	–0.242	0.004	–0.079	0.008	–0.089	0.006	5885	8	4.22	0.02	7.543	0.267
HIP 85042	–0.001	0.013	0.034	0.012	0.015	0.004	5694	5	4.41	0.02	6.662	0.617
HIP 8507	–0.046	0.006	–0.114	0.012	–0.096	0.006	5725	6	4.49	0.02	3.625	0.943
HIP 87769*	0.063	0.010	0.005	0.006	0.000	0.006	5807	6	4.40	0.02	5.145	0.687
HIP 89650	–0.031	0.007	–0.057	0.014	0.000	0.005	5841	5	4.44	0.02	3.824	0.755
HIP 9349	0.050	0.015	–0.042	0.015	0.009	0.007	5810	8	4.50	0.02	1.429	0.758
HIP 95962**	–0.001	0.010	0.047	0.012	0.023	0.005	5806	5	4.44	0.02	3.820	0.776
HIP 96160	0.020	0.004	–0.059	0.012	–0.053	0.007	5781	8	4.50	0.02	2.165	0.779